

UCLA

UCLA Previously Published Works

Title

Geotechnical reconnaissance findings of the October 30 2020, Mw7.0 Samos Island (Aegean Sea) earthquake

Permalink

<https://escholarship.org/uc/item/53f0r889>

Journal

Bulletin of Earthquake Engineering, 20(14)

ISSN

1570-761X

Authors

Ziotopoulou, Katerina
Cetin, Kemal Onder
Pelekis, Panagiotis
[et al.](#)

Publication Date

2022-11-01


DOI

10.1007/s10518-022-01520-x

Peer reviewed



Geotechnical reconnaissance findings of the October 30 2020, Mw7.0 Samos Island (Aegean Sea) earthquake

Katerina Ziotopoulou¹ · Kemal Onder Cetin² · Panagiotis Pelekis³ · Selim Altun⁴ · Nikolaos Klimis⁵ · Alper Sezer⁴ · Emmanouil Rovithis⁶ · Mustafa Tolga Yilmaz² · Achilleas G. Papadimitriou⁷ · Zeynep Gulerce² · Gizem Can² · Makbule Ilgac² · Elife Cakir² · Berkan Soylemez² · Ahmed Al-Suhaily² · Alaa Elsaied² · Moutasem Zarzour² · Nurhan Ecemis⁸ · Berna Unutmaz⁹ · Mustafa Kerem Kockar⁹ · Mustafa Akgun¹⁰ · Cem Kincal¹⁰ · Ece Eseller Bayat¹¹ · Pelin Tohumcu Ozener¹² · Jonathan P. Stewart¹³ · George Mylonakis^{14,15} 

Received: 16 August 2022 / Accepted: 14 September 2022
© The Author(s) 2022

Abstract

On October 30, 2020 14:51 (UTC), a moment magnitude (M_w) of 7.0 (USGS, EMSC) earthquake occurred in the Aegean Sea north of the island of Samos, Greece. Turkish and Hellenic geotechnical reconnaissance teams were deployed immediately after the event and their findings are documented herein. The predominantly observed failure mechanism was that of earthquake-induced liquefaction and its associated impacts. Such failures are presented and discussed together with a preliminary assessment of the performance of building foundations, slopes and deep excavations, retaining structures and quay walls. On the Anatolian side (Turkey), and with the exception of the Izmir-Bayrakli region where significant site effects were observed, no major geotechnical effects were observed in the form of foundation failures, surface manifestation of liquefaction and lateral soil spreading, rock falls/landslides, failures of deep excavations, retaining structures, quay walls, and subway tunnels. In Samos (Greece), evidence of liquefaction, lateral spreading and damage to quay walls in ports were observed on the northern side of the island. Despite the proximity to the fault (about 10 km), the amplitude and the duration of shaking, the associated liquefaction phenomena were not pervasive. It is further unclear whether the damage to quay walls was due to liquefaction of the underlying soil, or merely due to the inertia of those structures, in conjunction with the presence of soft (yet not necessarily liquefied) foundation soil. A number of rockfalls/landslides were observed but the relevant phenomena were not particularly severe. Similar to the Anatolian side, no failures of engineered retaining structures and major infrastructure such as dams, bridges, viaducts, tunnels were observed in the island of Samos which can be mostly attributed to the lack of such infrastructure.

Keywords Reconnaissance · Samos earthquake · Liquefaction · Lateral spreading · Slopes · Retaining structures · Foundations · Seismic performance

1 Introduction

On October 30, 2020 14:51 (UTC), a moment magnitude (M_w) of approximately 7.0 (United States Geological Survey, USGS (2020); European-Mediterranean Seismological Centre EMSC) earthquake occurred in the Aegean Sea north of Samos Island, Greece. The epicenter of the earthquake (N 37.8881°, E 26.7770°) was approximately 10 km north of Avlakia in Samos Island, and 23 km south of Doganbey in Izmir, with a focal depth of 17 km (AFAD). This paper aims to present the findings of field and desk studies performed by both Hellenic and Turkish geotechnical reconnaissance teams after the earthquake, and to discuss major conclusions drawn based upon these. Investigations of various aspects of the earthquake are available in literature (e.g. Akinci et al. 2021, Akkar et al. 2021, Askan et al. 2021, Binici et al. 2022, Cetin et al. 2021; 2022, Demir and Altioik 2021, Evelpidou et al. 2021, Ganas et al. 2021, Kalligeris et al. 2021, Kiratzi et al. 2021, Lentas et al. 2022, Makra et al. 2020; 2021, Mavroulis et al. 2022, Nuhoglu et al. 2021, Onat et al. 2022, Plicka et al. 2021, Toprak et al. 2022, Yakut et al. 2021).

Hellenic and Turkish geotechnical reconnaissance teams were mobilized in the field to collect and document perishable geotechnical data immediately after the event. In response to this event, the members of the Middle East Technical University, Earthquake Engineering Research Center (METU-EERC) along with several other research teams from Ege and Eylul Universities, as well as the Izmir Institute of Technology visited the region to investigate the effects of the earthquake. The reconnaissance study covered a large area, starting from Dilek Peninsula in the southwest, all the way up to Izmir Bornova in the northeast. Local reconnaissance teams mobilized to the area immediately after the event and METU team as of 3rd of November to collect and document perishable data in the form of ground deformations, liquefaction manifestations, possible failure or non-failure performances of soil, rock slopes and retaining structures. On the island of Samos, geotechnical reconnaissance was performed in two phases. Initially and a week after the earthquake, geotechnical engineers from the US and Greece were deployed between the 7th and 9th November 2020 as part of the Hellenic Association's for Earthquake Engineering (HAEE/ETAM) and GEER reconnaissance effort, and covered the northern part of the island and part of the southern part focusing on both structural and geotechnical damage (as discussed in HAEE - Vadaloukas et al. 2020). At a later phase and two months after the earthquake, a team of geotechnical engineers and geophysical testing experts from the University of Patras were deployed between the 19th and 21st December 2020 to obtain site information at selected locations in Samos that had been identified as key during the reconnaissance efforts in-between the two trips.

Discussions presented in this paper will focus on the documentation and the preliminary assessment of (i) performance of building foundations, (ii) seismic soil liquefaction and induced ground failures, (iii) performance of slopes and deep excavations, and (iv) performance of retaining structures and quay walls on both Samos and the Anatolian side for each case. As will be notable throughout the paper, with the exception of the Bayrakli region where significant and detrimental site effects (as discussed by Cetin et al. 2021) were observed, no major geotechnical effects were observed on the Anatolian side in the form of foundation failures, surface manifestation of liquefaction and lateral soil spreading, rock falls/landslides, failures of deep excavations, retaining structures, quay walls and subway tunnels.

On the island of Samos, evidence of liquefaction, lateral spreading and damage to quay walls in ports were observed on the northern side. Despite the proximity to the fault (about

10 km), and the significant amplitude/duration of shaking, the associated liquefaction phenomena were not pervasive, which suggests marginal liquefaction. It is also unclear whether the damage to quay walls was due to liquefaction of the underlying soil, or merely due to the inertia of those structures in conjunction with the presence of soft (yet not necessarily liquefied) foundation soil. A number of rock falls/landslides were observed; yet, again, the relevant phenomena were not particularly severe. Like in the Anatolian side, no failures of engineered retaining structures and major infrastructure such as dams, bridges, viaducts, tunnels were observed. This can be mostly attributed to the lack of such infrastructure on the island of Samos.

2 Performance of foundation systems

Foundation systems performed reasonably well on both sides of the Aegean Sea. Residential buildings were investigated in the center of Urla, Cesme, Kusadasi, Gumuldu, Izmir-Konak, Izmir-Bayrakli regions on the Anatolian side. Amongst them, no failures were identified that could be characterized as foundation-induced, i.e. as would have been evident by excessive total or differential settlement or tilting, or bearing capacity exceedance. Indicative pictures of satisfactory foundation performances are shown in Fig. 1. Most importantly, no foundation-induced structural failure mechanisms were observed or reported for the collapsed or heavily damaged buildings in Bayrakli and Bornova districts. For residential structures up to 7–9 stories, foundation systems were mostly identified as

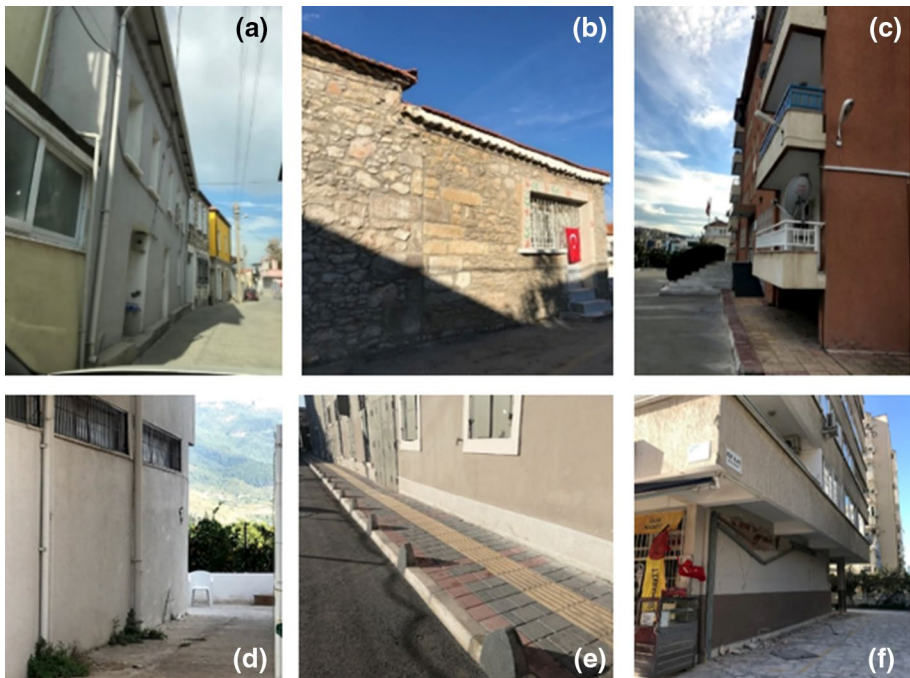


Fig. 1 Indicative cases of satisfactory foundation performance on the Anatolian side: **a** Urla, **b** Cesme, **c** Kusadasi, **d** Gumuldu, **e** Izmir Konak, and **f** Izmir Bayrakli

Fig. 2 Two-way combined footing system (grid spread footing foundation) of one of the heavily damaged buildings in Bayrakli, whose collapse is not foundation induced



Fig. 3 200 m high Twin Folkart Towers in Bayrakli supported on a piled raft system. No earthquake-induced damage was identified or reported for such foundation systems

two-way combined footings or individual footings with strip beams. Mat foundations are not very common for these low to mid-rise buildings belonging to pre-1995 period, despite the soft nature of underlying foundation soils. Figure 2 illustrates the foundation system of one of the fully collapsed buildings in Bayrakli whose collapse is not foundation induced. The recent development of high-rise buildings (Fig. 3) has, however, introduced the increasingly common use of piled raft systems. Barrette (rectangular pile) elements have been used in the foundation of these high-rise buildings. Additionally, in recent residential developments in Mavisehir, ground improvement applications in the form of jet grouting

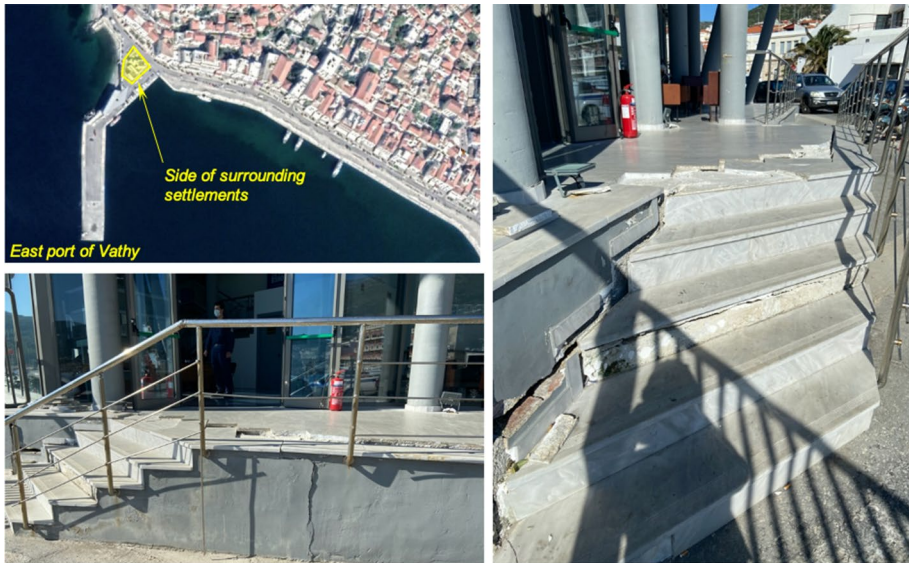


Fig. 4 Damage observed around the Port authority building in Vathy, Samos (location: $37^{\circ}45'27.0''$ N $26^{\circ}58'15.4''$ E). The cracks indicate soil settlement/distortion around the building which remained intact and functioning 8 days after the earthquake

and rammed aggregate piers have been widely used. Similarly, no foundation-induced deformations were observed at these sites.

On the island of Samos, no foundation failures were observed in the visited areas, with the possible exception of structural damage due to lateral spreading (see later Sect. 3). Figure 4 illustrates the Port authority building at the Eastern port of Vathy, where the observed damage patterns indicate a satisfactory piled foundation performance. Indeed, despite cracks and settlements around the building, the structure per se remained intact and was operating normally eight days after the earthquake when the HAEE/ETAM team inspected the site. At this point, it remains unclear whether these settlements are related to liquefaction, dynamic compaction, or failure of the retaining wall and an associated overall displacement of the backfilled soil (see Sect. 5 on the performance of the quay wall at the same site.)

2.1 Earthquake-induced liquefaction manifestations and induced ground failures

This section presents observations regarding the presence or lack of surface manifestations of earthquake-induced soil liquefaction in the form of sand boils and ejecta, excessive settlement, and lateral spreading. Along the Aegean coasts of Anatolia and inland, with the exception of Gulbahce, no surface manifestation of seismic soil liquefaction triggering was observed or reported. As shown in Fig. 5, evident by the USGS susceptibility map released immediately after the event, there were liquefaction susceptible regions where no surface manifestation of soil liquefaction was observed. USGS classified the area as one where liquefaction would be significant in severity and spatial extent. On the other hand, indications of liquefaction phenomena were observed on the island of Samos (and possibly in

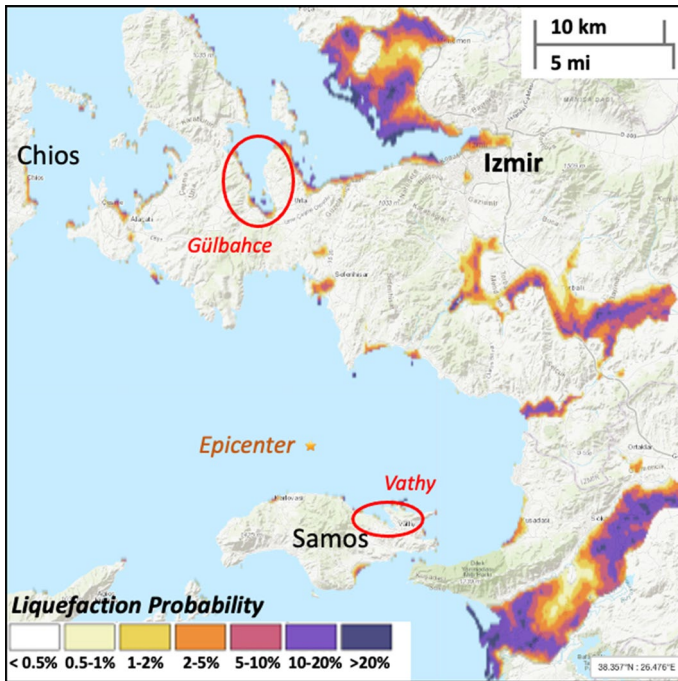


Fig. 5 USGS liquefaction susceptibility map released after the event showing liquefaction probability in the region surrounding the epicenter (not necessarily associated with the source at hand). The red ellipses indicate the only locations where evidence of liquefaction manifestation was identified

the port of the island of Chios located 100 km to the north-west of Samos; see Fig. 5) and its nearshore alluvial deposits in particular, despite the fact that the accompanying effects were not destructive.

Starting with the Anatolian side, as presented in Fig. 5, potentially liquefiable sites and shores were visited, and the lack of surface manifestation of soil liquefaction triggering was documented as no sand boils or displacements were identified. However, a number of surface manifestations were documented in Gulbahce-Izmir and Samos Island indicating the triggering of soil liquefaction, which will be discussed next (Fig. 6).

2.2 Gulbahce/Izmir

Consistent with the USGS susceptibility predictions, 45–50 km away from the rupture, along the shores of the Icmeler and Gulbahce districts, sand boils were observed, as shown in Fig. 7a through d. These sites were close to the Gulbahce fault zone, and documented artesian pressures along with hot water springs which are known to be present at these sites, which are also believed to have contributed to the observed soil ejecta formation. Figure 8 illustrates the results of grain size distribution analyses performed on soil samples retrieved from the sand ejecta. As can be seen, all samples were uniform and within the bounds typically delineated as liquefiable uniform soils.



Fig. 6 Selected photographs indicating no earthquake-induced soil liquefaction manifestation near-shore: **a** and **b** shores of Gumulduur city ($38^{\circ}04'30.9''$ N $26^{\circ}58'32.7''$ E/ November 3rd 2020/11:03 and $38^{\circ}03'30.6''$ N $27^{\circ}00'38.3''$ E/November 3rd 2020/10:30 respectively), **c** shores of Cesme ($38^{\circ}20'54.5''$ N $26^{\circ}27'07.6''$ E/ November 3rd 2020/09:54), and **d** shore of the Seferihisar district ($38^{\circ}05'11.5''$ N $26^{\circ}51'39.7''$ E / November 3rd 2020/11:31)



Fig. 7 Surface manifestations of earthquake-induced soil liquefaction in the form of sand boils at shores of Icmeler and Gulbahce district: **a** $38^{\circ}20'18.4''$ N $26^{\circ}38'51.0''$ E, **b** $38^{\circ}18'37.3''$ N $26^{\circ}40'47.1''$ E, and **c-d** 38.338088 N, 26.647763 E

2.3 Samos Island

Liquefaction has been historically manifested in various locations in Greece, particularly in many of its islands (Papathanasiou et al. 2005, 2010—Fig. 9). In the eastern Aegean Sea, the most recently recorded case of liquefaction was the one in Kos during the Bodrum-Kos $M_w = 6.6$ earthquake of 2017 (Papathanasiou et al. 2018). No liquefaction case histories have been recorded for Samos prior to this earthquake. The

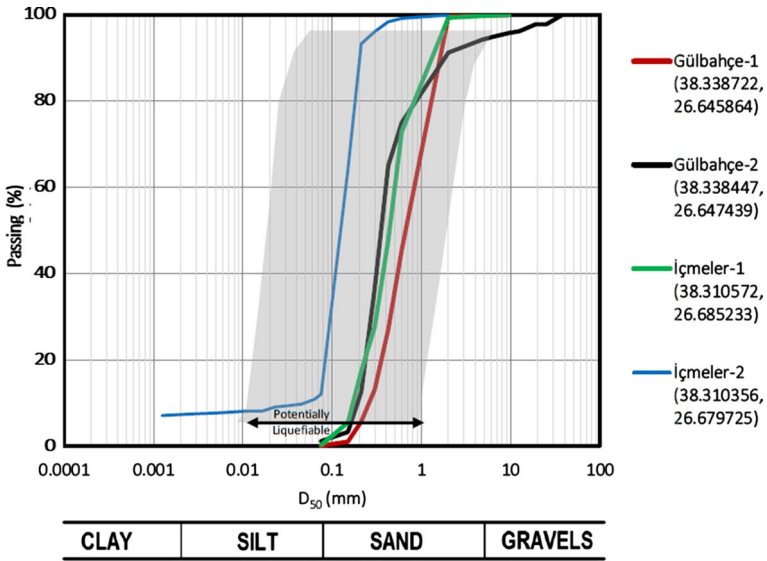


Fig. 8 Grain size distribution curves of sand ejecta obtained from Gülbahçe, along with the bounds of typically liquefiable non-uniform soils

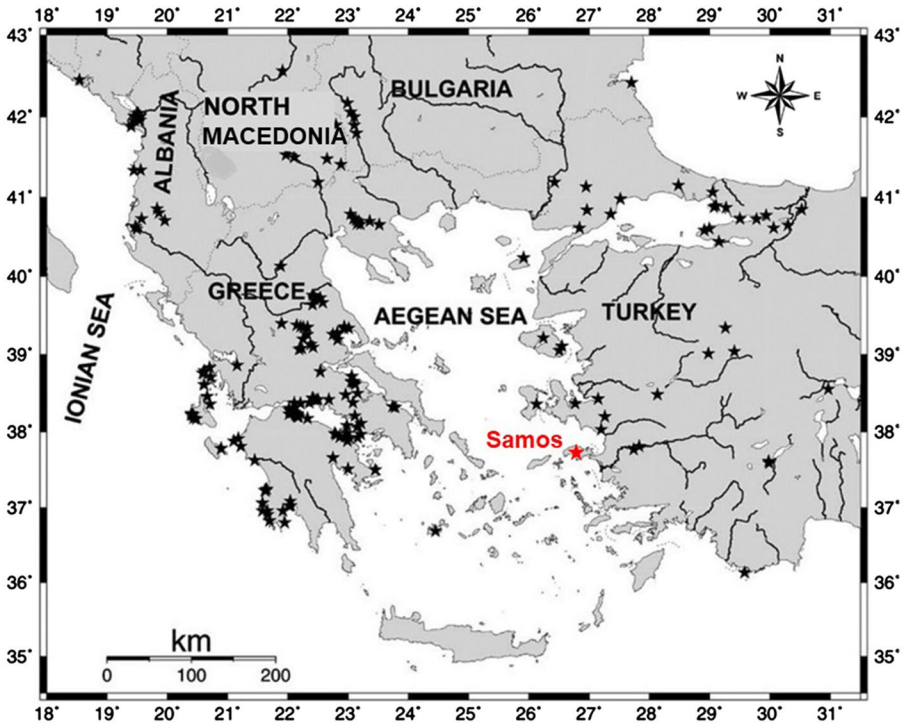


Fig. 9 Map of historical liquefaction occurrences in the broader Aegean region from 1509 to 2008 AD (after Papathanasiou et al., 2005, 2010)

reconnaissance team visited several locations along the northern and southern shores of the island. No liquefaction-related damages were observed along the southern coasts. In the north, liquefaction-induced sand boils and ejecta, as well as lateral spreading, were observed in one location (Malagari in the gulf of Vathy), while liquefaction is also suspected to be the leading cause behind the failure of some quay walls in the ports of Vathy and Karlovasi. Additional possible causes of quay walls failures referring to the large inertia of those structures, in conjunction with the presence of soft (yet not necessarily liquefied) foundation soil should not be excluded. Structural damages, compatible with lateral spreading of the foundation soil were observed in three buildings in the location of Vyrsopepsia in Karlovasi.

Manifestation of earthquake-induced liquefaction in the free field was observed in the area of Malagari, north-west from the town of Vathy, capital of the island of Samos. Specifically, the reconnaissance team located nearshore surface manifestations of liquefaction in the form of sand ejecta of grey color. As can be seen in Fig. 10, by the time the HAEE/ETAM team visited the site of interest (8 days after the earthquake), the ejecta had been slightly distorted due to the passage of vehicles. Nevertheless, the sand boils and their ejecta alongside with

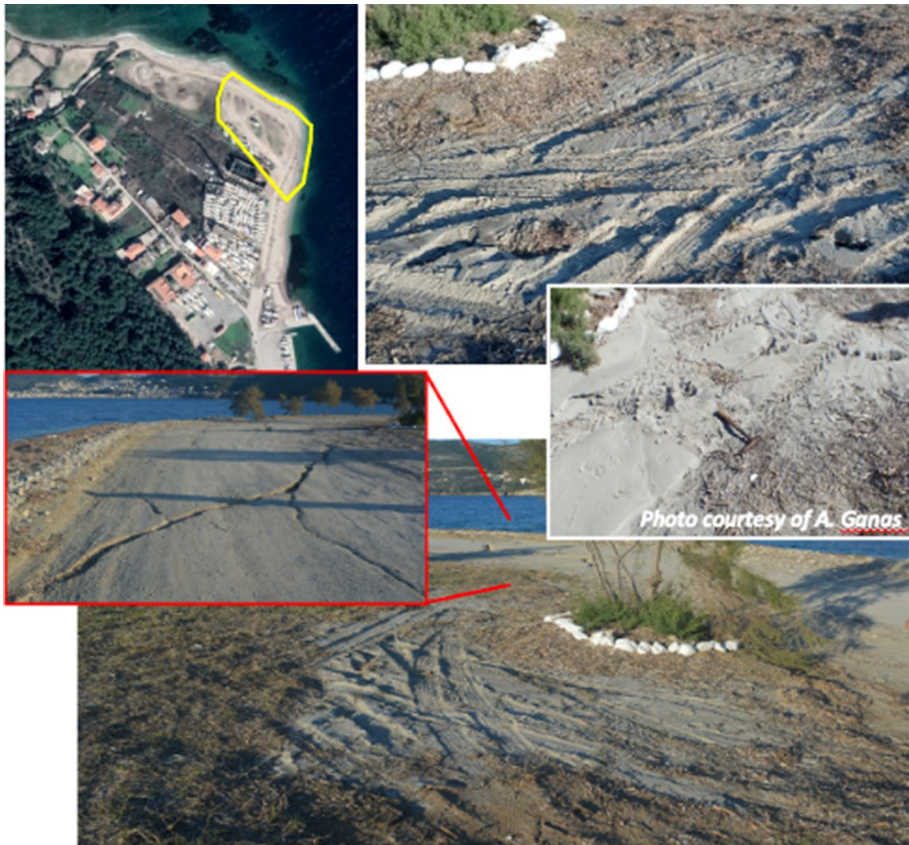


Fig. 10 Surface manifestations of earthquake-induced soil liquefaction in the form of sand boils in Malagari (location: $37^{\circ}45'24.6''$ N $26^{\circ}57'28.8''$ E—aerial imagery from 3001 ft) [photos taken by the HAEE/ETAM reconnaissance team and Dr. A. Ganas from NOA]

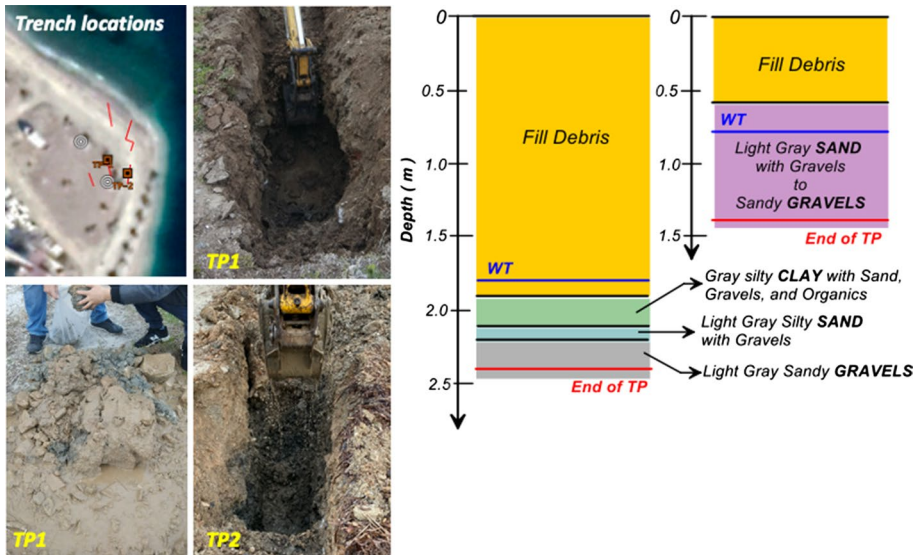


Fig. 11 Trenching at the Malagari liquefaction site and rough stratigraphy resulting from it

their broader extent were still easily visible and distinguishable. In the same area, ground cracks compatible with a lateral spreading mode of failure were observed and are emphasized in the inset of Fig. 10. The combination of the aforementioned with a free face to water, like in Malagari, eases the process, but lateral spreading has been manifested also in case histories with no free face (e.g. Balboa Boulevard failure during the 1994 Northridge earthquake—e.g. Stewart et al. 1996, Pretell et al. 2020). Trenching and soil sampling at two locations at the Malagari site were performed, which yielded two rough cross-sections and three grain size distributions for samples at three distinct depth intervals at the site illustrated in Figs. 11 and 12 respectively. The fines portion in all three samples was found to be non-plastic.

Shear wave velocity measurements performed after the earthquake using geophysical methods such as MASW (Professor Panagiotis Pelekis—20th December 2020) in the Malagari area that was affected by liquefaction yielded a time-averaged shear-wave velocity in the upper 30 m of the site $V_{s30}=215$ m/sec. The distribution of shear wave velocity V_s with depth is shown in Fig. 13. There are no borehole SPT or CPT data available at this site and the only relevant information is that from the Port of Malagari (West side of Vathy gulf) and borehole BH5 (Fig. 33). The geologic map of Samos (Fig. 13, but also Fig. 32) indicates that the Malagari site has alluvial deposits featuring plain deposits of clayey-sandy material, loam, sand, pebbles and gravels, which are potentially liquefiable when saturated. This particular site, where liquefaction was undoubtedly manifested, can be studied as a case history of either True Negative or True Positive liquefaction manifestation after more data are obtained and processed.

Lateral spreading effects were also evident through structural damage at other nearshore locations in the northern part of the island. Specifically, Figs. 14 and 15 illustrate three buildings and their location close to the north shore of the island, in the neighborhood Vyrsodepsia in Karlovasi. No surface manifestation of liquefaction was identified nearby, but the ground cracking crossing the street pavement and running through the buildings (the two in Fig. 16 are about 70 m inland and the one in Fig. 17 is about 20 m inland), in combination with the level/mildly sloping ground, the shallow water table, and the free face to the sea are all compatible with the hypothesis of lateral spreading.

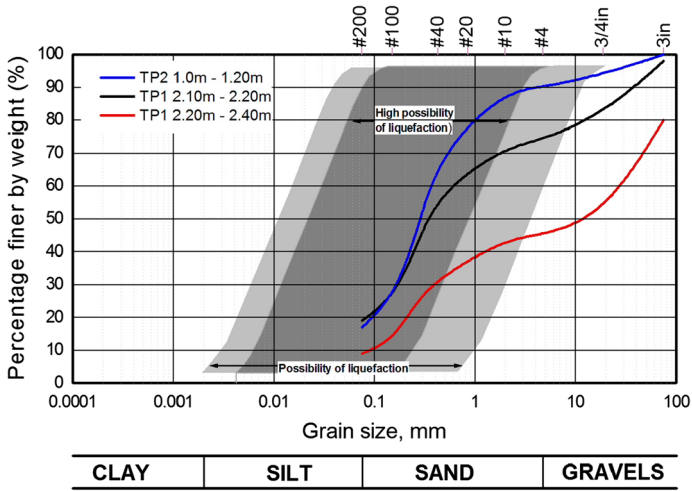


Fig. 12 Grain size distributions of three samples retrieved from different depths at the two trenching locations at the Malagari liquefaction site, along with the bounds of typically liquefiable non-uniform soils. The fines were found to be non-plastic (NP). (Geographic coordinates are provided in Fig. 10)

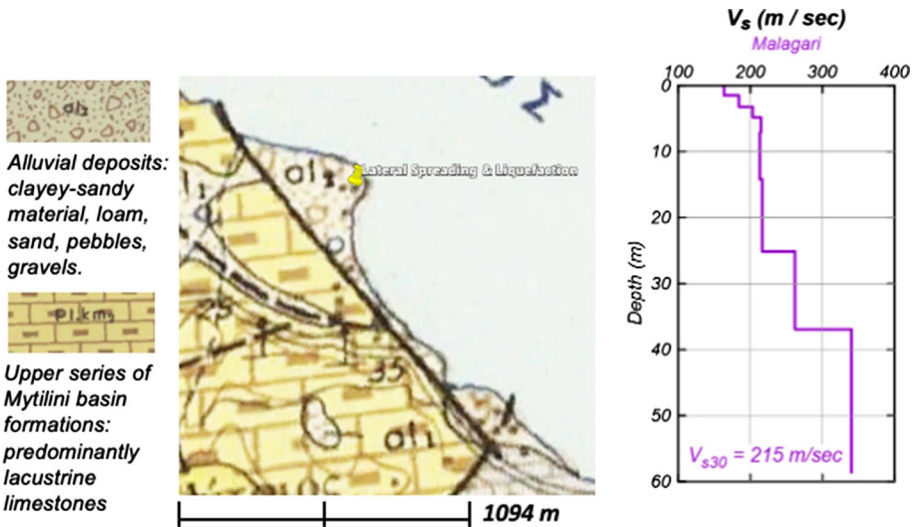


Fig. 13 Geologic map of Malagari indicating alluvial deposits and shear wave velocity profile at Malagari down to a depth of 60 m. (Geographic coordinates are provided in Fig. 10)

3 Performance of slopes and deep excavations

3.1 Performance of slopes in anatolia

In Anatolia, a limited number of rockfalls were observed by the benches of highways, one of which is illustrated in Fig. 18. Some potential and existing landslide sites were also inspected, but no signs of seismically induced movements were documented and are thus

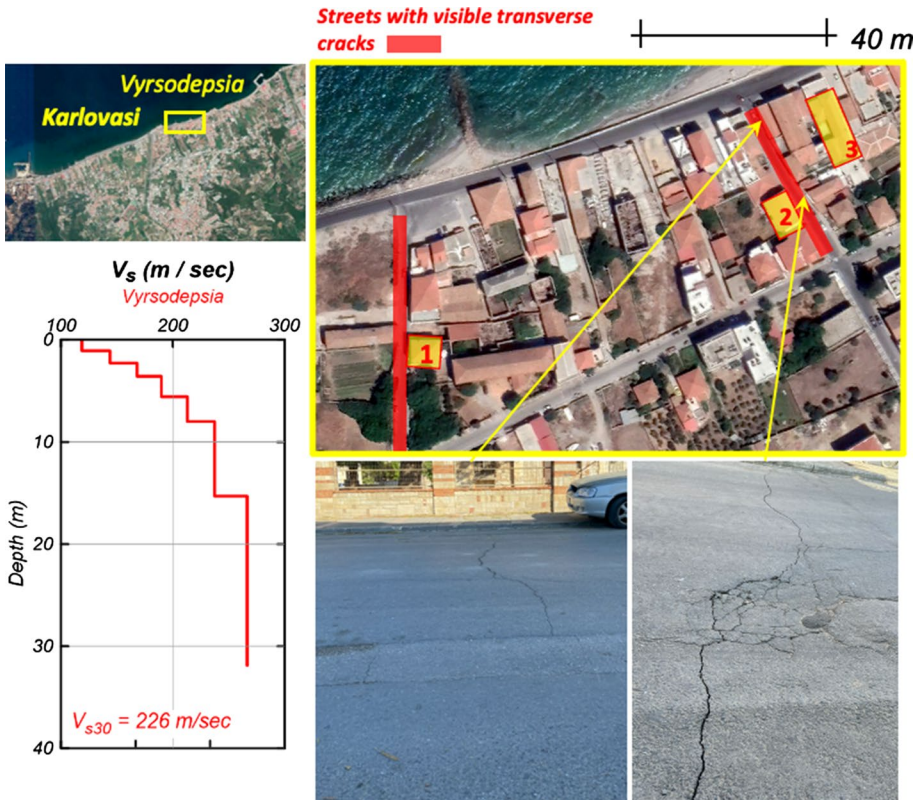


Fig. 14 Plan view of Karlovasi and the Vyrsodepsia neighborhood with buildings likely affected by lateral spreading towards the seafront alongside with shear wave velocity profile of the area down to a depth of 30 m (aerial close up at 1382 ft, 37o47'57.94" N, 26o42'23.27" E). The enumerated buildings are individually shown in Figs. 16 and 17

not presented herein. Furthermore, the highways were investigated and no proof of any seismically induced damage both on the highways or on the shoulder slopes was found, as shown in Fig. 19.

4 Performance of slopes in Samos

A series of minor-to-moderate slope failures and rockfalls were identified during the earthquake reconnaissance, mainly in the northern part of the island of Samos. The areas with nearby slope failures which are marked in a Google Earth map (Fig. 20) were located mainly by the reconnaissance team of HAEE/ETAM. The exact coordinates of these failures are also listed in Table 1, while some additional cases reported in Lekkas et al. (2020) and HSMGE (2020) are also shown. A brief description and representative photos are given below for some of these cases.

A weathered rock slide was recorded at a steep slope close to Avlakia region (Fig. 21), which caused a temporary closure of the road. The main geological formations in the above area are marbles with intercalations of schist (Cetin et al. 2021). However, the road access

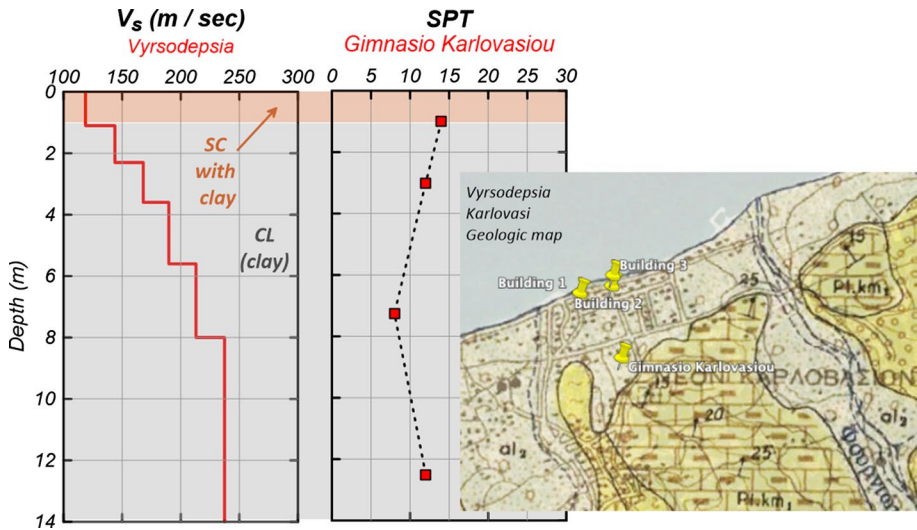


Fig. 15 Shear wave velocity profile down to a depth of 14 m alongside with SPT blow count information from the nearest borehole at the High School of Karlovasi (Gymnasium). Locations are shown in inserted geologic map

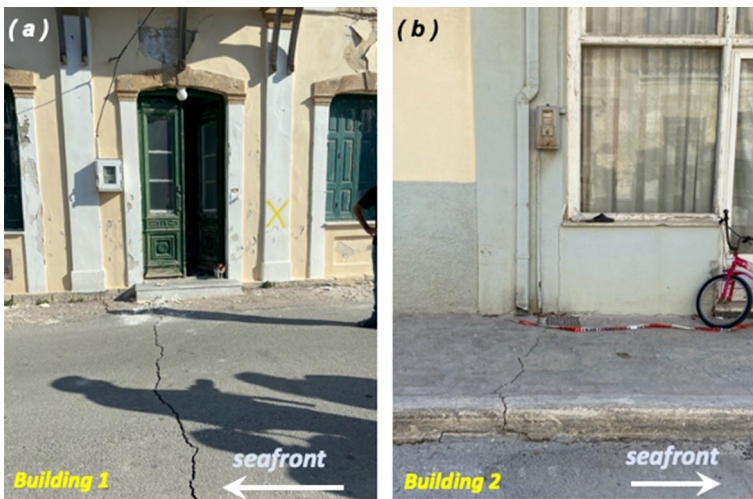


Fig. 16 Buildings likely affected by lateral spreading towards the seafront in the neighborhood of Vyrsopepsia in Karlovasi **a** 37°47'57.6" N 26°42'12.5" E and **b** 37°47'59.3" N 26°42'20.0" E [photos taken by the HAEE/ETAM reconnaissance team]

was quickly recovered after a few days by temporary restraining measures with large concrete blocks placed at the slope toe (Lekkas et al. 2020). Detachments of sandy marls and marly limestones were recorded very close to a residential building in Kokkari region (Fig. 22), while lighter failures referring to rockfalls and detachments of limestones, were observed close to the villages of Potami and Koumeika (Fig. 23a and b respectively). Slope



Fig. 17 Building affected by lateral spreading towards the seafront in the neighborhood of Vyrsopepsia in Karlovasi ($37^{\circ}48'01.1''$ N $26^{\circ}42'20.6''$ E). The cracks observed running across the building indicate 3-5 cm of movement [photos courtesy of Prof. K. Antonopoulos]

Fig. 18 Fallen rock blocks in the Anatolian side ($37^{\circ}53'50.4''$ N $27^{\circ}22'06.2''$ E)



Fig. 19 Selected indicative views of highway cuts with no signs of slope instability ($38^{\circ}17'31.6''$ N $26^{\circ}40'14.6''$ E)

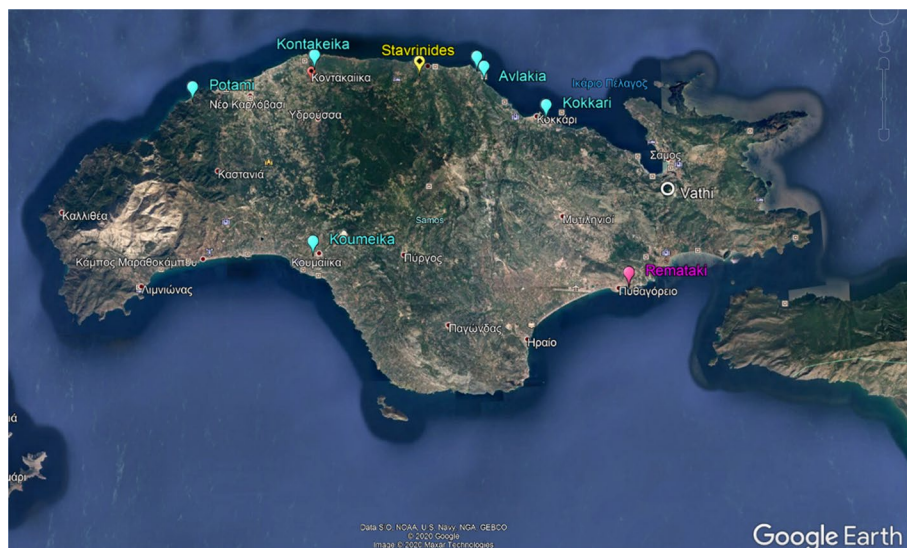


Fig. 20 Geographical distribution of slope-type failures located by the HAEE/ETAM reconnaissance team during the visit on 7th November, 2020 (cyan pins). Additional sites with light slope failures recorded by Lekkas et al. (2020) (magenta pin) and HSGME (2020) (yellow pin) are also shown

failures of similarly low intensity were also recorded by other reconnaissance teams. These include limestone segments falls in the area of Remataki (next to Pythagorio—Fig. 23c) or rockfalls close to the village Stavrinides (Fig. 23d).

In the village of Kontakeika, extended ground cracks (openings of about 10–20 cm) were observed that were compatible with the mobilization of a larger, albeit very mild, slope or could be more broadly characterized as seismically-induced secondary ground failures (Fig. 24). The HAEE/ETAM team did not locate other similar indications of ground cracking in the near or extended vicinity of Kontakeika so, at this point in time, it is challenging to draw conclusions regarding the nature of this observation. According to local engineers, the Municipality of Samos had repaired the pavement in that particular location several times in the past, which suggests a pre-existing creeping landslide that could have been reactivated by the earthquake. The cracks extended on both sides of the street through soft soil formations (Fig. 24).

4.1 Deep excavations

The new downtown district (Bayrakli-Bornova) of Izmir (Turkey) is founded on the sedimentary basin, where the heavily affected region from the earthquake is situated. Numerous high-rise buildings are constructed on these soft soil conditions. Many of them have multi-story basements, thus deep excavation systems had to be designed reaching depths of 20 m. Due to the shallow ground water level and the proximity to the shoreline, typical shoring systems contain mostly diaphragm walls laterally supported by pre-stressed anchors. In the sedimentary district, two well-monitored deep excavation systems, which were under construction in the three months leading up to the earthquake, were shaken (Fig. 25). Both of these systems reached a depth of about 9 m while their satisfactory performance was recorded by

Table 1 Locations of the slope failures in Samos recorded by the HAEE reconnaissance team during in-situ visit on 7th November, 2020

Region with nearby slope failure	Coordinates of the inspected slope failure	
	Latitude (°)	Longitude (°)
Avlakia	37°47'48.0" N	26°51'27.7" E
Potami (close to Karlovasi)	37°47'17.6" N (approx.)	26°40'00.5" E (approx.)
Tsampou beach (close to Avlakia)	37°48'08.0" N	26°51'17.2" E
Kokkari	37°46'49.9" N	26°53'35.0" E
Koumeika (south Samos)	37°42'33.7" N	26°44'52.9" E
Kontakeika	37°48'01.6" N	26°44'29.5" E
Remataki	37°41'26.51" N	26°56'43.38" E
Stavrinides	37°47'48.52" N	26°48'49.04" E

the installed monitoring system (Fig. 26). No failure or relaxation of pre-stressing loads on anchors was measured/observed. These observations are also supported by inclinometer measurements taken before and after the earthquake. The measurements suggest that the lateral displacements (illustrated in Fig. 26) accumulated during the earthquake were less than 2 mm. No relevant data are available from Samos (or any of the nearby islands) in Greece, since there are no similarly deep excavations constructed.

5 Performance of retaining structures and quay walls

5.1 Retaining structures

There are no reported failures of engineered retaining structures in Turkey. During the reconnaissance studies, a limited number of tilted and/or partially collapsed safety walls were observed, as documented in Fig. 27. Additionally, no damage on retaining walls due to seismic shaking was encountered during the reconnaissance inspections of the sites in the south of İzmir province, as shown in Fig. 28. These stone walls are generally used to provide a buffer area between the cut slopes and highway to obstruct or retard the shallow failures to reach the highway. Regardless of the height of these stone walls, no seismically-induced deformations or failure was observed on the highway connecting Menderes to Gumuldur. No damage was found on the sides of spillway channels of the dams in the region. No sign of any structural damage was likewise observed on these walls (Fig. 29). Figure 30 shows the sidewalls of the river canal in Sığacık Marina, hit by the tsunami after the earthquake. No structural distress can be observed on these walls, which suggests that the severity of shaking was modest despite its proximity to the rupture. Additionally, no signs of liquefaction or permanent deformations were reported.

The lack of failed or damaged retaining systems is unsurprising, since this event produced less severe shaking intensities than the design basis levels. More specifically, the seismic stability of retaining walls has been analyzed in design assessments by considering a seismic coefficient (k_h) equal to half of peak ground acceleration (PGA), or 20% of spectral acceleration for a short period range (or, for a period of 0.2 s) of the design spectrum. Hence, for İzmir, a seismic coefficient value of 0.2 ($k_h = 0.2$) has been



Fig. 21 **a** Snapshot of Avlakia rockslide from a video recorded during the failure (source: <https://www.cnn.gr/ellada/story/240726/seimos-samos-vinteo-apo-katolisthisi-sta-aylakia>) **b** aerial photograph of the slide 2 weeks after the earthquake (courtesy of I.N. Spyrou and Prof. K. Ziopoulou 37°47'48.0" N, 26°51'27.7" E), and **c** a closer view of the rockslide illustrating the rock formation more clearly (picture by HAEE/ETAM reconnaissance team)



Fig. 22 Detachment of sandy marls and marly limestones recorded very close to a residential building in the Kokkari region (photos taken by the HAEE/ETAM reconnaissance team, 37°46'49.9" N, 26°53'35.0" E). Vertical open cracks are visible, clearly susceptible to detachment and toppling

generally presumed in seismic analysis and design considering a seismic hazard level expressed by the return period of 475 years for being exceeded, following the seismic hazard map of Turkey that took effect after the year 1996. The recorded PGA during the seismic event and spectral amplitudes on response spectra of accelerograms point out a less severe shaking intensity than that considered for seismic design of the retaining walls. No relevant data are available for the Samos and Chios islands.

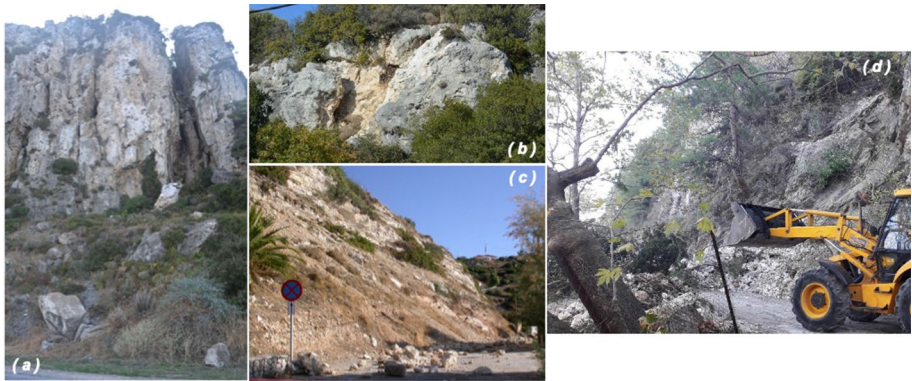


Fig. 23 **a** Rockfalls observed at the road network close to the village of Potami (photo taken by the HAEE/ETAM reconnaissance team, $37^{\circ}47'17.6''$ N, $26^{\circ}40'00.5''$ E), **b** Detachment of limestone segments close to the village of Koumeika (photo taken by the HAEE/ETAM reconnaissance team, $37^{\circ}42'33.7''$ N, $26^{\circ}44'52.9''$ E), **c** Falls of limestone segments on a provincial road in the Remataki region (photo reported by Lekkas et al. 2020), and **d** Slope failure close to the village of Stavrinides (photo reported by HSGME 2020)



Fig. 24 Ground and pavement cracks in the village of Kontakeika (Samos), indicative of the mobilization of an extended but mild slope or more broadly characterized as seismically-induced secondary ground failures. The cracks extended on both sides of the street through soft soil formations. Arrows in the figure explain the relative location of the cracks

5.2 Quay walls

This section focuses on the performance of the main ports of Samos Island, and to a lesser extent on the performance of the main port of Chios island, where a member of the HAEE/ETAM reconnaissance team happened to be present when the earthquake struck. As far as the Anatolian side is concerned, no excessive settlement or other earthquake-induced damage was identified along the Anatolian coastal line (e.g.,



Fig. 25 **a** Pre-earthquake view of shored deep excavation located in the “new downtown” district in Bayrakli-Bornova ($37^{\circ}53'50.4''$ N $27^{\circ}22'06.2''$ E), and **b** Plan view of the site under discussion

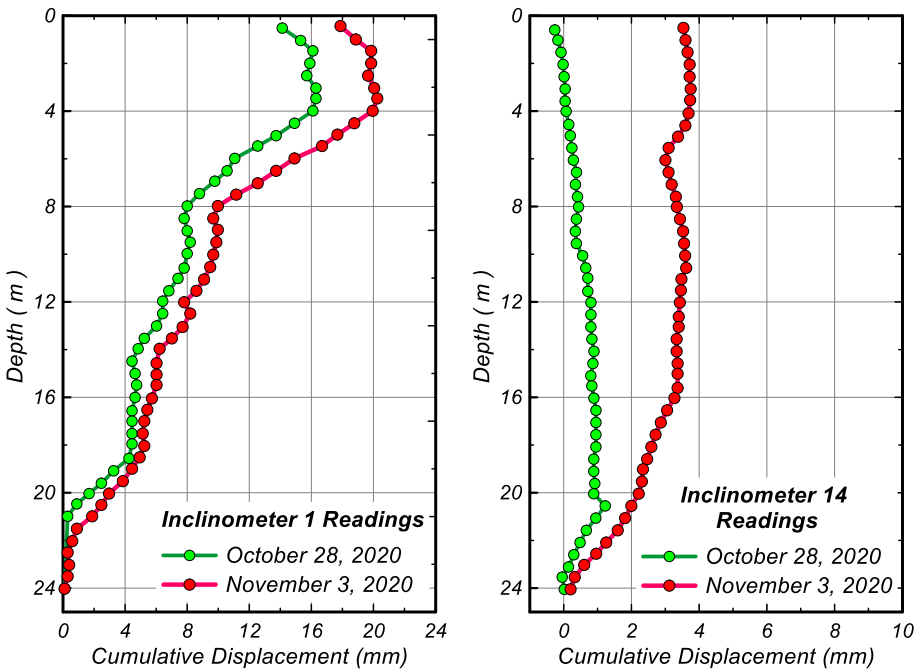


Fig. 26 Inclinometer data covering the period of earthquake shaking, at a 9 m-deep excavation in Izmir, Turkey, supported by diaphragm walls

rubble mound breakwaters, armor layer of any rubble mound protection). Additionally, inspected gravity-type quay walls, composed of concrete blocks and constructed in fishery harbors and commercial and cruise ports, and floating piers in the Marinas showed no earthquake-induced damage, despite their relatively old age.

The ports of Vathy and Karlovasi (Fig. 31) are the two main gates of ferry connection between Samos and the mainland, as well as the rest of the islands in NE Aegean

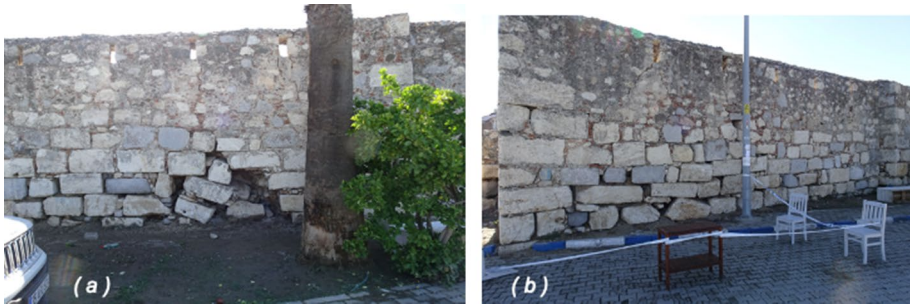


Fig. 27 Deformed and cracked safety wall at **a** $38^{\circ}11'40.93''$ N $26^{\circ}47'3.47''$ E/14:16/October 31, 2020, and **b** $38^{\circ}11'40.34''$ N $26^{\circ}47'3.22''$ E /14:22/October 31, 2020

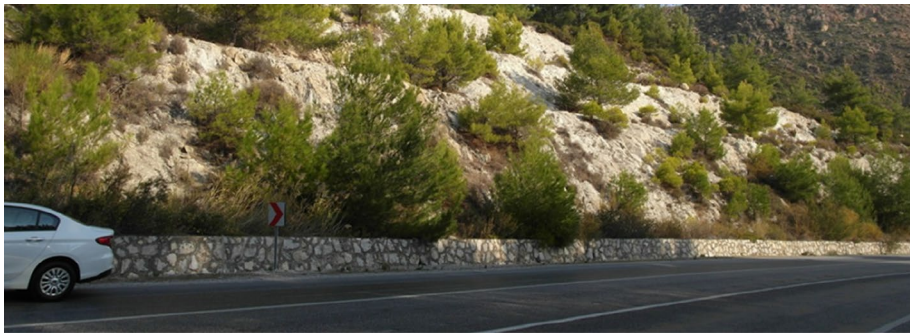


Fig. 28 Short, stoned retaining walls on the toe of the highway cuts between Menderes and Gumuldur in the south of İzmir city center

Sea and the Dodecanese islands. Both ports are situated at the northern part of Samos and suffered damage due to the earthquake. There is also a smaller port, Kokkari, which is located in-between the Vathy and Karlovasi ports. That port was also affected by the earthquake; however, the economic impact of the damage was less important relative to that of the other two ports. At the southern part of the island, there are some other ports, at Pythagorio, Iraion, and Marathokampos bay, that were less affected by the earthquake (HAEE/ETAM 2020).

5.3 Ports of Vathy

In Vathy (Fig. 31 top right), port installations are split between two facilities: the eastern (old) port and the western (new) port—also known as the “Malagari” port, due to its proximity to the Malagari area that is situated about 1 km northwest (for liquefaction effects at Malagari, see Figs. 10 and 11 alongside with the corresponding text). The eastern (old) port is founded on alluvial deposits consisting mainly of clayey-sandy materials, sands, gravels and pebbles. This is shown in Fig. 32, where part of the geological map of Samos published by HSGME, is presented. In the same Figure, a number of boreholes on the specific geology are superimposed, as collected by the Hellenic reconnaissance team. Although all boreholes have been drilled through the same alluvial deposits, there is a clear



Fig. 29 a Wall on the end of spillway chute of Kavakdere Dam, and side walls of spillways of b Urkmez Dam, c Tahtalı Dam, and d Gumuldur Dam



Fig. 30 Sidewalls of the river canal in the Sığacık Marina where no displacements were observed (Photo: Courtesy of Gurel Özdemir). (38°11'33.86"N 26°47'4.07"E 14:16 / 31.10.2020)

pattern that can be observed as one moves alongshore, from east (BH 1) to west (BH 4 and BH 5): if continuous, the layer of sandy silt or silty sand (ML-SM) emerges at shallower depths and also gets thicker (Fig. 33). However, given the distance between Vathy and Malagari as well as the relative depth and thickness of the ML-SM layer in each location, it is also possible that this is not the same layer across the sites. The associated SPT blow counts are extremely low (essentially zero), which indicates very low strength and high compliance. As the associated materials are non-plastic and saturated, this provides evidence of susceptibility to liquefaction.

The jetty of the eastern (old) port experienced extensive longitudinal and transverse open cracks—several centimeters wide—whilst the backfill behind the quay wall experienced a subsidence that locally exceeded 50 to 60 cm (Fig. 34). In Fig. 34b, traces of gravels and sand are visible behind the quay wall. These might be remnants of ejecta partially washed out by the tsunami. The presence of ejecta could be the result of liquefaction of a very loose sandy silt layer located 15 to 18 m deep, right beneath the backfill material (Fig. 34a). Similar observations of ejecta behind quay walls have been made in many previous earthquakes (Professor G. Bouckovalas—*personal communication*), even in the absence of any native liquefiable soil layer. As such, any observed ejecta may be due to liquefaction and wash out of a loosely deposited fine silty-sand phase which fills the voids of a typically much coarser backfill gravel skeleton that does not participate in the load-carrying capacity of the wall (Professor G. Bouckovalas—*personal communication*). This could explain the lack of excessive displacements and rotations of the wall towards the sea. Construction records from the said ports and further investigations can elucidate this further.

The previous observations and arguments are further strengthened by the magnitude of the recorded accelerations. It is indeed questionable whether the accelerations recorded on that site were strong enough to force the liquefiable loose sandy silt get ejected from a depth of 15 to 18 m to the surface. These doubts are reinforced by information from the opposite side of the port, i.e. the western (new) port where the very loose to very soft layer of silty sand to sandy silt (SM-ML) does not provide any evidence of severe/extensive liquefaction. This seems to be the case, despite the layer at hand being thicker and shallower, as well as similar to that in the Malagari site (situated about 400 m NW from the new port). On the basis of the above data, it is possible that the upper 15 m of borehole BH1 is material that has been superimposed over the layer of very loose sandy silt, which most likely is the preexisting natural layer (often found in ports and bays). This material appears highly deformable, with very low bearing capacity, so that cracks and deformations might have already existed. Discussions

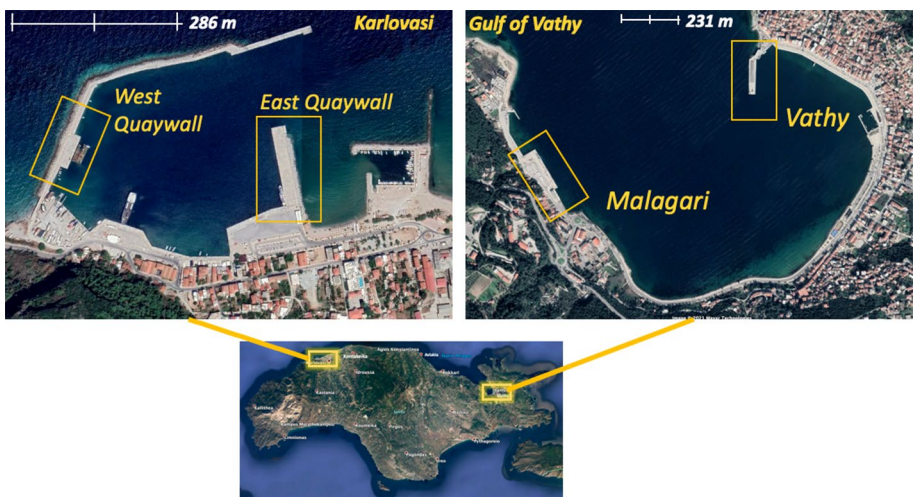


Fig. 31 Satellite images providing an overview of ports of interest in Samos where significant earthquake damage was observed. Annotations indicate the names assigned for ease of reporting herein

with the local port engineers, revealed that the pavement was mildly cracked prior to the earthquake (Mrs. Sechioti, *personal communication*). If this is indeed the case, then most probably the cracks might have simply further opened/intensified after the earthquake at hand. Also, it could not be verified whether the traces of sand and gravel shown in Fig. 34b are (i) ejecta from a distinct layer that liquefied, (ii) ejecta from a finer sand portion in the coarser skeleton of the backfill, or (iii) just a natural product of friction and bouncing between the backfill material and the quay wall following their detachment. Given the preliminary observations and the experience from other earthquakes in the broader area and their effects on similar infrastructure, it is more likely that the latter two explanations are the most plausible ones.

The western (new) port of Vathy, Malagari, is the commercial port where passenger and car ferries are mainly serviced, as well as smaller ships. The total length of the coastal quay wall is about 500 m along the NW–SE direction. Some basic geological features and relevant geotechnical data have already been presented in Fig. 32. Based on these data, a remediation study and the quay wall and the port infrastructure was put together on December 2017 (Triton, 2017). Figure 35 shows the quay walls, as part of the recent rehabilitation project (Triton, 2017). According to Triton (2017), the jetty of Malagari is a gravity structure made of overlapping layers of artificial boulders (5 in each column). On the crown there is an in-situ cast superstructure. The quay wall is founded on a rockfill prism, whose external side along the seaside is protected by natural boulders. A representative sketch of a typical cross-section of the quay wall is depicted in Fig. 35 (Triton, 2017). The technical issues encountered before the earthquake mainly relate to scouring of the quay walls which can be attributed to leakage of the relief prism and upstream backfill material, leading to substantial subsidence behind the quay walls, opening of cracks parallel and transversely to the sea front, and a mild rotation of some quay wall columns towards the sea. The remedial measures outlined in the 2017 report were probably in progress (yet, not completed) when the earthquake struck.

Figure 36a illustrates a view of the pre-existing open joints between the quay wall and the backfill material and the subsidence of the backfill material behind the quay wall about 3 years ago (Triton 2017), and its comparison to Fig. 36b which illustrates its condition immediately after the earthquake (HAEE/ETAM reconnaissance report 2020).



Fig. 32 Detail of the geological map of Samos, according to the Hellenic Survey of Geology and Mineral Exploration (HSGME 2020). A number of boreholes are shown, carried out on the same geological formation (al2)

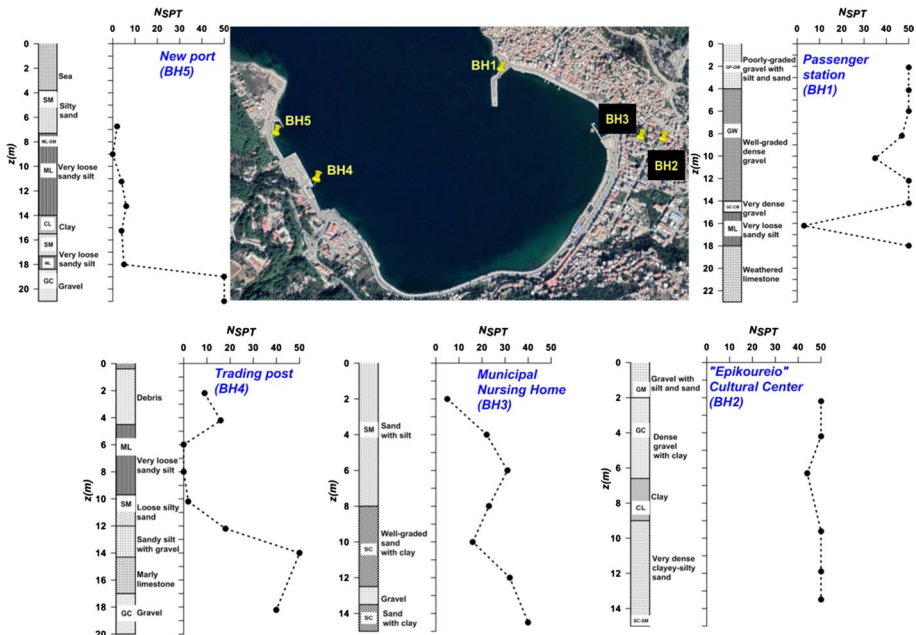


Fig. 33 Four geotechnical borehole logs (BH1, BH2, BH3, BH4) alongshore from the eastern (old) port to the western (new) port at Vathy (courtesy of G. Milionis—modified by Em. Rovithis). One offshore borehole (BH5) at the NW edge of the new port (kindly provided by the Ministry for the Environment, Physical Planning and Public Works of Greece – modified by Em. Rovithis)

Interestingly, the earthquake damage observed is quite similar, but most probably intensified by the earthquake. At the time the site was visited by the HAEE/ETAM team, the construction operations in response to the Triton (2017) study were ongoing. Hauled construction materials did allow the team to delineate between those and any potential liquefaction-induced ejecta at the site. Nevertheless, given the geotechnical data liquefaction might have taken place on a rather limited scale and probably worsened the existing damage. In addition, the quay walls at this particular site are massive and consequently subject to large inertia forces mostly due to their own mass and not due to seismic earth pressures from the backfill. Consequently, it is likely that the quay walls at the Malagari port rotated somewhat outwards during the earthquake, thus widening any pre-existing gaps (Triton 2017) and also leading to some settlement of the backfill next to the wall. As such, it is rather unlikely that the present picture of the quay wall damage can be attributed entirely to liquefaction and dynamic settlement.

5.3.1 Port of Karlovasi

The Karlovasi port is second only to that of Vathy for the commercial and economic life of the island. Figure 31 illustrates a satellite view of the port and both its east and west quay walls. Karlovasi is founded on the same geological structure as Vathy, i.e., alluvial deposits consisting mainly of clayey-sandy materials, sands, gravels and pebbles. This is shown in Fig. 37, where part of the detailed geological map of Samos Island published by the Hellenic Survey of Geology and Mineral Exploration (HSGME), is presented. Available data

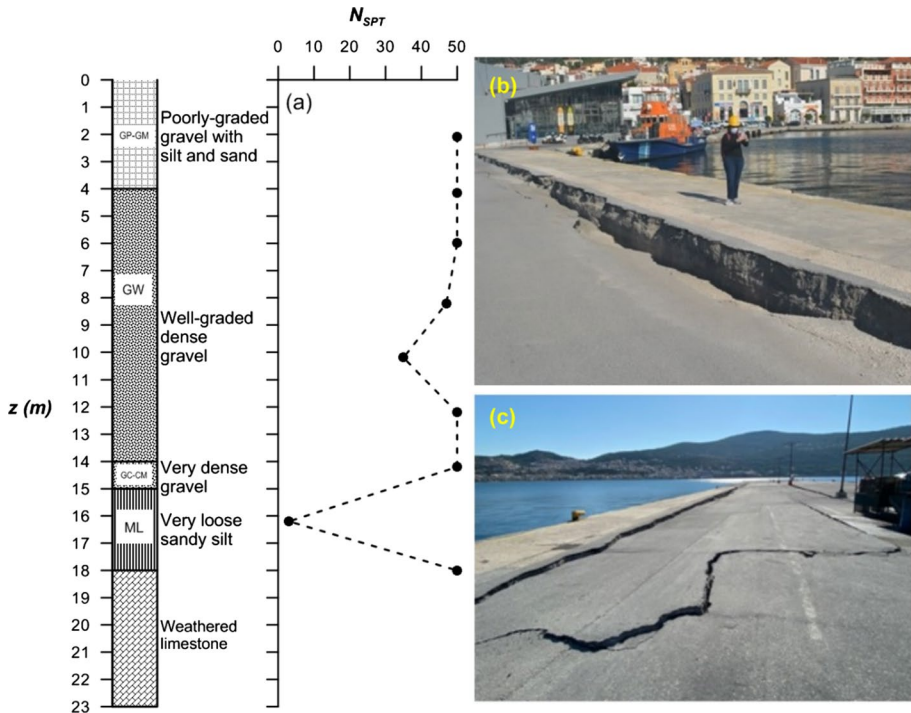


Fig. 34 a Crude log of borehole BH1 located at the jetty of the old port of Vathy, where the liquefiable layer of the very loose sandy silt layer is located at a depth of 15 m (data provided by G. Milionis—elaboration by Em. Rovithis) and SPT blow count with depth. b Subsidence of backfill material behind the quay wall at the eastern (old) port, measuring up to 60 cm. c 10–15 cm wide longitudinal and transversal open cracks, located on the pavement over the backfill material, in contact with the quay wall

from a borehole close to the high school of Karlovasi indicate that the soil consists of grey to grey-brownish medium stiff to stiff sandy clay of medium plasticity (excluding the top 1 m that consists of silty sand with a few gravels). The distance to the closest part of Karlovasi port (east quay wall) is about 2 km; therefore, it is difficult to extrapolate as to the subsoil in the port. However, based on the soil layering at Vathy, there is a possibility that the surficial layer of silty sand gets thicker near the seashore. This however, albeit generally true, cannot be reliably deduced without geotechnical data.

The port of Karlovasi suffered damage to both jetties, namely: subsidence of the backfill material (or the subsoil), mild tilting and displacement of the quay walls towards the sea, cracks (both transversely and parallel) to the quay walls. Also, grey-brown ejecta of sand-gravel mixture was found on the west quay wall, which possibly emerged through the cracks. Even in the absence of sufficient data to substantiate the occurrence of liquefaction, it appears that liquefaction is a reasonable scenario. This possibility is reinforced considering that the surface layer of grey-brownish silty sand identified at the high school area, seems to be continuing and getting thicker close to the sea shore. However, without additional geotechnical data, it is impossible to draw conclusions and this is only a hypothesis in accordance to the subsurface structure at Vathy. Last but not least, the construction details of each port need to be accounted for, since the placement of a backfill under “wet” or “dry” conditions can severely affect its dynamic response in seismic events. Figure 38

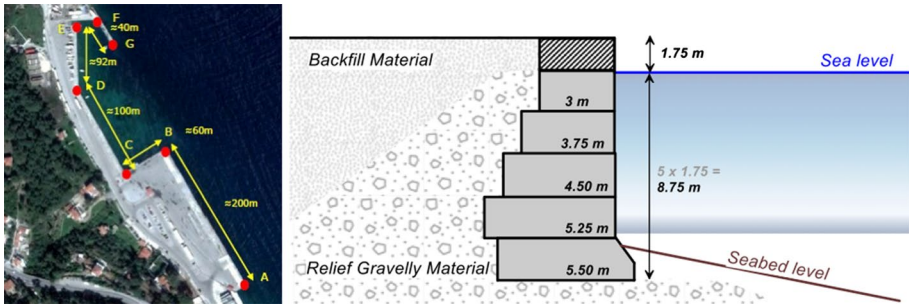


Fig. 35 Satellite view over infrastructure of the western Vathy port (Malagari) (Triton 2017) and typical cross-section of the quay wall of the new (Malagari) port of Vathy corresponding to section A–B (out-of-scale drawing, modified after Triton 2017)

illustrates both jetties (east and west), as well as ejecta observed on the western quay wall. Nevertheless, it is hard to tell whether the cracks and subsidence/tilting patterns are earthquake induced, or merely pre-existing gravity-induced effects.

5.3.2 Port of Kokkari

Kokkari is a small village in the northern part of Samos, situated about 10 km NW from Vathy. It has a small port mainly serving fishing boats and small yachts. The reconnaissance team of HEAA visited Kokkari and observed that the quay wall had suffered severe subsidence, 10 to 20 cm wide open cracks alongside the sea front, and mild tilting towards the sea, as shown in Fig. 39. It is unclear whether the deformations were pre-existing i.e.

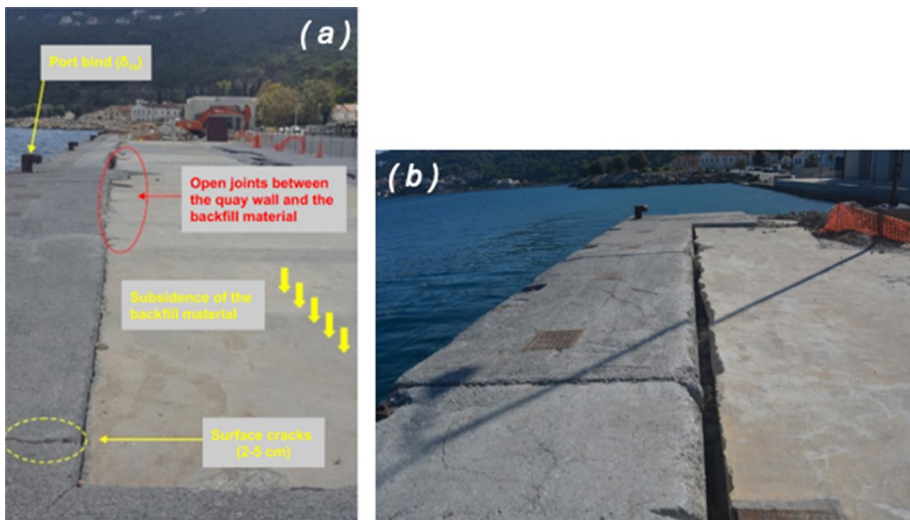


Fig. 36 View of the quay wall at new (Malagari) port, Vathy, from NW to SE direction: **a** photo taken 3 years before the earthquake (Triton 2017); **b** photo taken a few days after the earthquake (HAEE/ETAM reconnaissance report 2020)

due to the low quality of the quay wall construction and the lack of protection of its underwater part from scour. Problems related to low bearing capacity and differential settlements due to a soft and compressible surface soil layer at the foundation of the jetty cannot be excluded. However, no clear traces of liquefaction were detected following the earthquake.

5.3.3 Port of Chios Island

Earthquake-induced failures were also observed in the port of Chios island, situated approximately 80 km north of the fault, referring mainly to surface cracks of considerable width and depth (Fig. 40a), as reported in the post-earthquake preliminary report by Pelekis and Roumelioti (2020). At specific locations these cracks were about 10–15 cm wide and about 40 cm deep (Fig. 40b). Such type of failures in the port of Chios may indicate soil liquefaction that was marginally triggered during the earthquake, and ensuing lateral spreading effects towards the shoreline, as suggested by Pelekis and Roumelioti (2020). The existence of inclined strata below the filling material of the quay walls and pre-earthquake damage due to gravity loads (e.g. scour of its foundation) should be considered when interpreting the observed seismic behavior. The possibility of marginal triggering of soil liquefaction was reinforced following a series of MASW field tests, which revealed the existence of soft/low-strength surficial soil layers with shear wave propagation velocity of about 100 m/s. A preliminary V_s -based assessment of the safety factor against soil liquefaction (Andrus and Stokoe, 2000) revealed a potential triggering of the phenomenon during the $M_w=7.0$ event for PGAs above approximately 0.12 g (Fig. 40c).

6 Geotechnical performance of metro tunnels, bridges, viaducts, and highways

Metro tunnels, most of which were located within 10–20 m depths, occasionally in soil formations or weathered rock were reported to be in uninterrupted service after the event. Additionally, although Naldoken and Zafer Payzin viaducts, and Turan and Egemak bridges are located on relatively soft and/or potentially liquefiable soils, no geotechnical or foundation-induced damage was reported at these bridges, viaducts, along with highways.

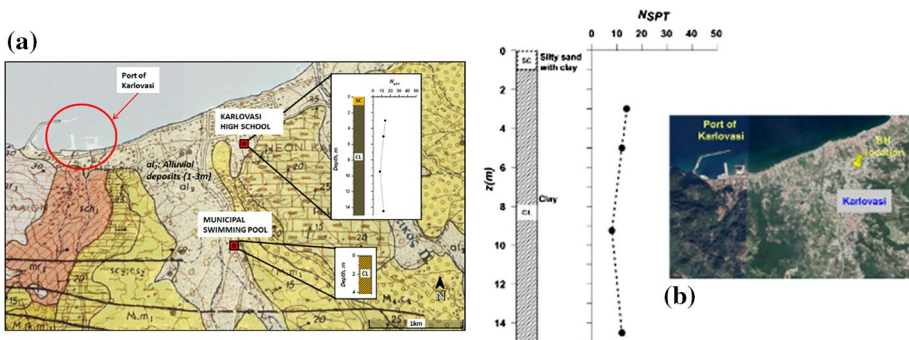


Fig. 37 **a** Part of the detailed geological map of Samos Island, published by the Hellenic Survey of Geology and Mineral Exploration (HSGME 2020) with the location of two (2) geotechnical boreholes on the same geological formation (a12). **b** Borehole log next to the High School of Karlovasi (Gymnasium), at a distance of about 2 km from the east quay wall of the port and 550 m from the seafront

All the above pertain to the Anatolian side. Due to lack of relevant infrastructure, no such effects were observed in Samos and Chios islands in Greece.

7 Major findings and conclusions

From a geotechnical engineering point of view, consistent with the proximity to the source and elevated intensity levels, the majority of the documented permanent ground deformation, liquefaction and slope failure cases are concentrated in Samos Island. However, equally importantly, their lack was also documented on the Anatolian side. While this can be mainly attributed to the distance from the source, more research is needed to identify the relevant factors of safety. In what follows, the major geotechnical performance observations from the Anatolian side after this event are listed:

- (i) Many residential buildings have been investigated in the center of Urla, Cesme, Kusadasi, Gumuldur, Izmir-Konak, Izmir-Bayrakli regions. No foundation-induced failures, evident by excessive total or differential settlement or tilting, or bearing capacity exceedance, were mapped or reported.
- (ii) Along the Aegean coasts of Anatolia and inland, no surface manifestation of seismic soil liquefaction triggering was observed or reported, despite the presence of liquefaction susceptible alluvial basins.
- (iii) However, at 45–50 km away from the rupture, along the shores of Icmeler and Gulbahce districts, sand boils were observed. These sites were close to Gulbahce fault zone, and the presence of documented artesian pressures along with hot water springs are believed to contribute to the observed soil ejecta formation.

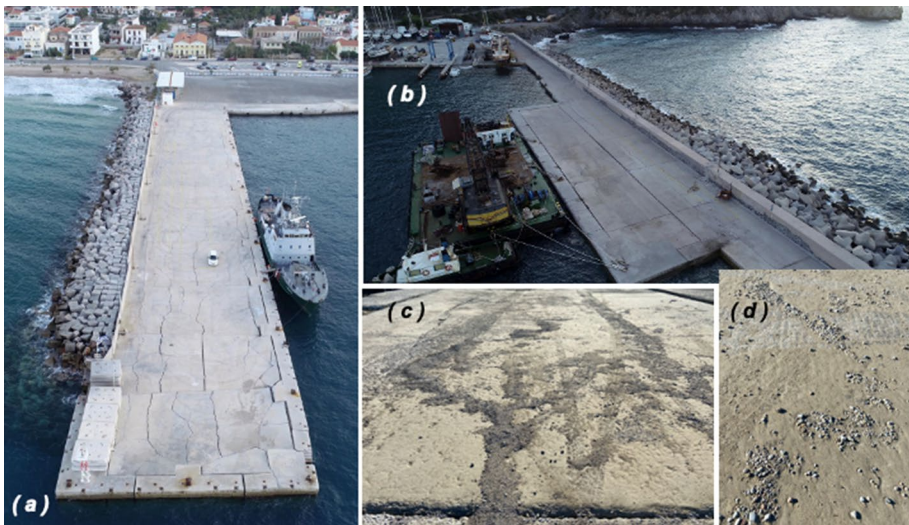


Fig. 38 **a** East quay wall of Karlovasi port, **b** west quay wall of Karlovasi port, **c** ejecta on the west quay wall, presumably the product of liquefaction occurrence, and **d** a detailed view of the ejecta, brownish to grey color, mostly sandy and silty with some gravels (aerial photographs courtesy of I.N. Spyrou and Prof. K. Ziotopoulou)

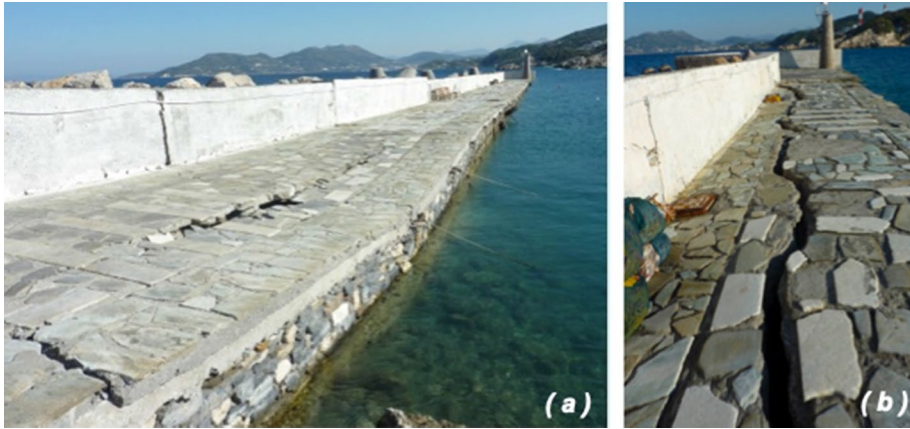


Fig. 39 **a** Differential subsidence of the quay wall of Kokkari port with wide open cracks alongside and transversely, **b** close view of an open crack of 10 to 15 cm alongside the sea front (HAEE/ETAM 2020)

- (iv) A few rock falls were observed by the benches of highways. Some potential and existing landslide sites were visited, but no signs of seismically induced movements were documented. Similarly, deep excavation support systems in Izmir were reported to have performed well.
- (v) There are no reported failures of engineered retaining structures in Turkey. During the reconnaissance studies, a limited number of non-engineered tilted and/or partially collapsed safety walls were observed.
- (vi) Similarly, despite tsunami-induced damage in port facilities, no geotechnical engineering related permanent ground deformations or failures are reported for quay walls.
- (vii) Metro lines in Izmir were reported to be in uninterrupted service after the event, and no permanent deformations or failures were reported.

The geotechnical performance observations from the Samos and Chios islands after the earthquake event of the 30th of October, 2020 are:

- (i) Although located only about 10 km from rupture, the towns of Vathy and Karlovasi in Samos were rather lightly affected by the earthquake, with relatively few collapsed or heavily damaged buildings. With the possible exception of a small set of structures (e.g. at Vyrsopepsia near Karlovasi) which were damaged due to lateral soil spreading, no earthquake-induced damage was observed on foundations.
- (ii) Several manifestations of liquefaction were observed along the north coast of Samos, including Vathy (Malagari site) and possibly Karlovasi (Vyrsopepsia) and the ports. Nevertheless, the associated phenomena were not spectacular, which indicates that liquefaction was manifested but not in a pervasive manner. This is surprising given the intensity ($PGAs > 0.2 g$) and duration ($\approx 9 s$ in records at Vathy; see Cetin et al. 2021) of ground motion in combination with the nearshore alluvial deposits. The precise dimensions of the liquefied zones is hard to establish without detailed site investigations.

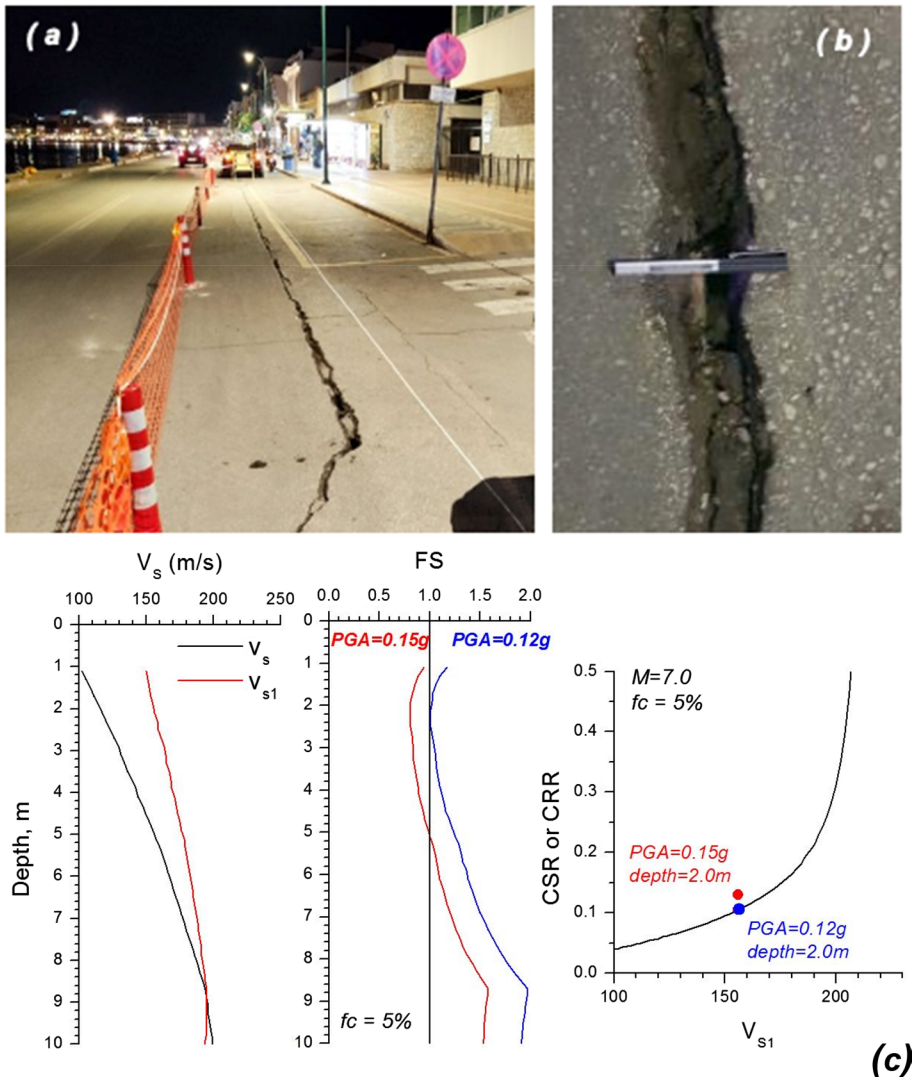


Fig. 40 **a** Earthquake-induced surface cracks parallel to the quay wall front in the port of Chios, **b** close-up view of 10–15 cm wide and 40 cm deep surface cracks, and **c** preliminary Vs-based assessment of the safety factor against soil liquefaction at the depth of 2 m for PGA equal to (i) 0.15 g and (ii) 0.12 g (Pelekis and Roumelioti, 2020)

- (iii) A number of landslides and rock falls occurred in the north part of Samos. Again, the relevant phenomena were not particularly severe and probably relate to precariously standing rocks and slopes. Such effects have been observed in other recent earthquakes in the regions at hand and elsewhere (Mylonakis et al. 2003, Margaris et al. 2008, 2010, Giarlelis et al. 2011, Nikolaou et al. 2014, Sextos et al. 2018)

- (iv) There are no reported failures of engineered retaining structures and other infrastructure (e.g. dams, bridges, viaducts, tunnels) in Samos or Chios. This can be mostly attributed to the lack of such infrastructure in the islands.
- (v) Port facilities in Vathy, Karlovasi and Kokkari were significantly affected by the earthquake, with considerable displacements/rotations of quay walls towards the sea, pavement cracks and backfill settlements behind the walls, and some signs of ejecta associated with liquefaction. Nevertheless, it is unclear if the primary source of those movements is soil liquefaction—or simply the significant inertia of those structures, in combination with the cyclic mobility of soft (mostly cohesive) soil layers under the walls, and the unilateral nature of loading and ensuing response.
- (vi) Significant movements, including cracks on the pavement, were observed on the quay wall in the port of Chios island, about 80 km from fault. Again, it is unclear whether the movement can be attributed to soil liquefaction or to the inertia of the quay walls per se.

As a final remark, it is noted that a number of key geotechnical parameters such as the extent of the liquefiable zones, seasonal variation of the elevation of the water table, artesian pressures etc. are hard to establish without detailed site investigations which lie beyond the scope of this work. Preliminary studies can be conducted using Vs30 values inferred from geologic and terrain-based proxies (Stewart et al. 2014).

Acknowledgements The authors are indebted to Professor George Bouckovalas of the National Technical University of Athens, Prof. Dr. Atilla Ansal of Ozyegin University, Istanbul, Prof. Dr. Ayfer Erkin of Istanbul Technical University, Prof. Dr. Bilge Siyahi of Gebze Technical University, Istanbul for their valuable review of this work, and their insightful comments that significantly improved many of the discussions presented herein, particularly those pertaining to the seismic performance of foundation systems and seismic response of port facilities. The authors would also like to deeply thank external contributors who kindly provided data and assistance with carrying out field measurements included in this paper. In this regard, George Milionis, Geologist, provided the boreholes log data for BH1, BH2, BH3 and BH4 shown in Figure 33 while the borehole log data for BH5 shown in the same figure was provided by Peggy Sechioti, employee of the Hellenic Ministry of Infrastructure and Transport. MASW field measurements by Prof. P. Pelekis were supported by Vasilis Christopoulos, laboratory member, and Paraskevi Paliatsa, postgraduate student, Civil Engineering Department, University of Patras. The members of Middle East Technical University, Ankara were partially funded by reconnaissance funds of METU, which is greatly appreciated. The authors are also thankful to Professor K. Antonopoulos and Gurel Ozdemir for sharing photographs from local earthquake damages, and to Dr. Prodromos Psarropoulos, who did reconnaissance work as member of the HAEE/ETAM geotechnical team, for sharing information. Their valuable contribution is gratefully acknowledged. Financial support to the U-Patras team was provided by HAEE/ETAM. Prof Katerina Ziotopoulou's field reconnaissance and participation was supported by the NSF-sponsored Geotechnical Extreme Events Reconnaissance (GEER) association. The work of the GEER Association, in general, is based upon work supported in part by the National Science Foundation through the Geotechnical Engineering Program under Grant No. CMMI-1826118. Any opinions, findings, and conclusions or recommendations expressed in this material are those of the authors and do not necessarily reflect the views of the NSF. Any use of trade, firm, or product names is for descriptive purposes only and does not imply endorsement by the U.S. Government. The GEER Association is made possible by the vision and support of the NSF Geotechnical Engineering Program Directors: Dr. Richard Fraszky and the late Dr. Cliff Astill. Last but not least, the authors are grateful to the anonymous reviewers who provided constructive feedback that improved the work.

Funding The authors have not disclosed any funding other than ad hoc financial support to specific co-authors.

Conflict of interest The authors have not disclosed any competing interests.

Open Access This article is licensed under a Creative Commons Attribution 4.0 International License, which permits use, sharing, adaptation, distribution and reproduction in any medium or format, as long as you give appropriate credit to the original author(s) and the source, provide a link to the Creative Commons

licence, and indicate if changes were made. The images or other third party material in this article are included in the article's Creative Commons licence, unless indicated otherwise in a credit line to the material. If material is not included in the article's Creative Commons licence and your intended use is not permitted by statutory regulation or exceeds the permitted use, you will need to obtain permission directly from the copyright holder. To view a copy of this licence, visit <http://creativecommons.org/licenses/by/4.0/>.

References


- Akinci A, Cheloni D, Dindar AA (2021) The 30 October 2020, M7.0 Samos Island (Eastern Aegean Sea) Earthquake: effects of source rupture, path and local-site conditions on the observed and simulated ground motions. *Bull Earthq Eng* 19(12):4745–4771
- Akkar S, Çağlar NM, Kale Ö, Yazgan U, Sandıkkaya MA (2021) Impact of rupture-plane uncertainty on earthquake hazard: observations from the 30 October 2020 Samos earthquake. *Bull Earthq Eng* 19(7):2739–2761
- Andrus RD, Stokoe KH II (2000) Liquefaction resistance of soils from shear-wave velocity. *J Geotech Geoenviron Eng* 126(11):1015–1025
- Askan A, Gülerce Z, Roumelioti Z et al (2021) The Samos Island (Aegean Sea) M7.0 earthquake: analysis and engineering implications of strong motion data. *Bull Earthq Eng*. <https://doi.org/10.1007/s10518-021-01251-5>
- Binici B, Yakut A, Canbay E et al (2022) Identifying buildings with high collapse risk based on Samos earthquake damage inventory in İzmir. *Bull Earthq Eng*. <https://doi.org/10.1007/s10518-021-01289-5>
- Cetin KO, Papadimitriou AG, Altun S, Pelekis P, Unutmaz B, Rovithis E, Akgun M, Klimis N, Askan GA, Ziotopoulou K, Sezer A, Kıncal C, İlgaç M, Can G, Çakır E, Söylemez B, Al-Suhaily A, Elsaid A, Zarzour M, Stewart J, Mylonakis G (2021) The role of site effects on elevated seismic demands and corollary structural damage during the October 30 2020, M7.0 Samos Island (Aegean Sea) Earthquake. *Bull Earthq Eng*. <https://doi.org/10.1007/s10518-021-01265-z>
- Cetin KO et al (2022) The site effects in İzmir Bay of October 30 2020, M7.0 Samos earthquake. *Soil Dyn Earthq Eng* 152:107051
- Demir A, Altıok TY (2021) Numerical assessment of a slender structure damaged during October 30, 2020, İzmir earthquake in Turkey. *Bull Earthq Eng* 19(14):5871–5896
- Evelpidou N, Karkani A, Kampolis I (2021) Relative sea level changes and morphotectonic implications triggered by the Samos earthquake of 30th October 2020. *J Mar Sci Eng* 9(1):40
- Ganas A et al (2021) Co-seismic and post-seismic deformation, field observations and fault model of the 30 October 2020 Mw= 7.0 Samos earthquake, Aegean Sea. *Acta Geophys* 69(3):999–1024
- Giarlelis C, Lekka D, Mylonakis G, Karabalis D (2011) The M6.4 Lefkada 2003, Greece, Earthquake: Response of a 3-Storey RC Structure on Soft Soil. *J Earthq Struct* 2(3):257–277
- HAEE – Vadaloukas G, Vintzileou E, Ganas A, Giarlelis C, Ziotopoulou K, Theodoulidis N, Karasante I, Margaris B, Mylonakis G, Papachristidis A, Repapis C, Psarropoulos PN and Sextos AG (2020) Samos Earthquake of 30th October, 2020. Preliminary Report of the Hellenic Association for Earthquake Engineering, Athens, Greece. <https://doi.org/10.13140/RG.2.2.22609.76644>
- Hellenic Survey of Geology and Mineral Exploration (H.S.G.M.E) (2020) Immediate response of HSGME after the 30 October 2020 Samos earthquake. Short note released on 31 Oct 2020 (in Greek)
- Kalligeris N, Skanavis V, Charalampakis M, Melis NS, Voukouvalas E, Annunziato A, Synolakis CE (2021) Field survey of the 30 October 2020 Samos (Aegean Sea) tsunami in the Greek islands. *Bull Earthq Eng* 1–33
- Kiratzis A, Papazachos C, Özacar A et al (2021) Characteristics of the 2020 Samos earthquake (Aegean Sea) using seismic data. *Bull Earthq Eng*. <https://doi.org/10.1007/s10518-021-01239-1>
- Lekkas E, Mavroulis S, Gogou M, Papadopoulos GA, Triantafyllou I, Katsetsiadou KN, Kranis H, Skourtsos E, Carydis P, Voulgaris N, Papadimitriou P, Kapetanidis V, Karakonstantis A, Spingos I, Kouskouna V, Kassaras I, Kaviris G, Pavlou K, Sakkas V, Karatzetou A, Evelpidou N, Karkani E, Kampolis I, Nomikou P, Lambriou D, Krassakis P, Fouvelis M, Papazachos C, Karavias A, Bafi D, Gatsios T, Markogiannaki O, Parcharidis I, Ganas A, Tsironi V, Karasante I, Galanakis D, Kontodimos K, Sakellariou D, Theodoulidis N, Karakostas C, Lekidis V, Makra K, Margaris V, Morfidis K, Papaioannou C, Rovithis E, Salonikios T, Kourou A, Manousaki M, Thoma T, Karveleas N (2020) The October 30, 2020 Mw 6.9 Samos (Greece) earthquake. *Newsletter of Environmental, Disaster and Crises Management Strategies*, 21, ISSN 2653–9454.

- Lentas K, Gkarlaouni CG, Kalligeris N et al (2022) The 30 October 2020, $M_w = 7.0$, Samos earthquake: aftershock relocation, slip model, Coulomb stress evolution and estimation of shaking. *Bull Earthq Eng* 20:819–851. <https://doi.org/10.21203/rs.3.rs-534400/v1>
- Makra K, Rovithis E, Riga E, Raptakis D, Pitolakis K (2020) A note on the strong ground motions recorded in Izmir (Turkey) during the October 30th, 2020 $M 7.0$ Aegean Sea earthquake: The role of basin effects. A non-peer reviewed preprint uploaded to ResearchGate (November 29, 2020). <https://doi.org/10.13140/RG.2.2.34517.65762>
- Makra K, Rovithis E, Riga E, Raptakis D, Pitolakis K (2021) Amplification features and observed damages in İzmir (Turkey) due to 2020 Samos (Aegean Sea) earthquake: identifying basin effects and design requirements. *Bull Earthq Eng* 19(12):4773–4804
- Margaris V, Papaioannou C, Theodoulidis N, Savvaïdis A, Klimis N, Makra K, Karakostas C, Lekidis V, Makarios T, Salonikios T, Demosthenus M, Athanasopoulos G, Mylonakis G, Papantonopoulos C, Efthymiadou V, Kloukinas P, Ordóñez I, Vlachakis V, and Stewart JP (2008) Preliminary report on the principal seismological and engineering aspects of the $M_w = 6.5$ Achaia-Ilia (Greece) earthquake on 8 June 2008. GEER Association Report No. GEER-013, Web report
- Margaris V, Athanasopoulos G, Mylonakis G, Papaioannou C, Klimis N, Theodulidis N, Savvaïdis A, Efthymiadou V, Stewart JP (2010) The 8 June 2008 $M_w 6.5$ Achaia-Elia, Greece Earthquake: Source Characteristics, Ground Motions, and Ground Failure. *Earthq Spectra* 26(2):399–424
- Mavroulis S, Ilgac M, Tunçağ M, Lekkas E, Püskülcü S, Kourou A... Karveas N (2022) Emergency response, intervention, and societal recovery in Greece and Turkey after the 30th October 2020, $M_w = 7.0$, Samos (Aegean Sea) earthquake. *Bull Earthq Eng* 1–23
- Mylonakis G, Voyagaki E, Price T (2003) Damage potential of the 1999 Athens, Greece, accelerograms. *Bull Earthq Eng* 1(2):205–240
- Nikolaou et al (2014) Geotechnical Aspects of the $M = 6.1$ January 27 and February 03, 2014, Cephalonia, Greece, Earthquakes. GEER Association Report No. GEER-034 Web report
- Nuhuğlu A, Erener MF, Hizal Ç, Kincal C, Erdoğan DŞ, Özdağ ÖC, Sezer A (2021) A reconnaissance study in Izmir (Bornova Plain) affected by October 30, 2020 Samos earthquake. *Int J Disaster Risk Reduct* 63:102465
- Onat O, Yön B, Öncü ME, Varolgüneş S, Karaşın A, Cemalgil S (2022) Field reconnaissance and structural assessment of the October 30, 2020, Samos, Aegean Sea earthquake: an example of severe damage due to the basin effect. *Nat Hazards* 112(1):75–117
- Pelekis P, Roumelioti Z (2020) Preliminary results of an autopsy at Chios port. Technical report of Patras University for TEE of Chios Island, Section of NE Aegean
- Papathanasiou G, Pavlides S, Christaras B, Pitolakis K (2005) Liquefaction case histories and empirical relations of earthquake magnitude versus distance from the broader Aegean region. *J Geodyn* 40:257–278. <https://doi.org/10.1016/j.jog.2005.07.007>
- Papathanasiou G, Valkaniotis S, Chatzipetros A, Pavlides S (2010) Liquefaction susceptibility map of Greece. *Bull Geol Soc Greece*. <https://doi.org/10.12681/bgsg.11314>
- Papathanasiou G, Valkaniotis S, Pavlides S (2018) The July 20, 2017 Bodrum-Kos, Aegean Sea $M_w = 6.6$ earthquake; preliminary field observations and image-based survey on a lateral spreading site. *Soil Dyn Earthq Eng* 116:668–680
- Plicka V, Gallović F, Zahradník J, Serpetsidaki A, Sokos E, Vavlas N, Kiratzi AA (2021) The 2020 Samos (Aegean Sea) $M7$ earthquake: a normal fault with rupture directivity and near surface slip explaining the tsunami generation and coastal uplift. *Earth and Space Science Open Archive ESSOAr*
- PreteLL RA, Ziotopoulou K, Davis C (2020) Numerical modeling of ground deformations at Balboa Blvd in the Northridge 1994 Earthquake. *ASCE J Geotech Geoenviron Eng*. [https://doi.org/10.1061/\(ASCE\)GT.1943-5606.0002417](https://doi.org/10.1061/(ASCE)GT.1943-5606.0002417)
- Stewart JP, Seed RB, Bray JD (1996) Incidents of ground failure from the 1994 Northridge earthquake. *Bull Seismol Soc Am* 86(1):300–318
- Stewart JP, Klimis N, Savvaïdis A, Theodulidis N, Zargli E, Athanasopoulos G, Pelekis P, Mylonakis G, Margaris B (2014) Compilation of a local vs profile database and its application for inference of vs30 from geologic- and terrain-based proxies. *Bull Seismol Soc Am* 104(6):2827–2841. <https://doi.org/10.1785/0120130331>
- Sextos A, De Risi R, Pagliaroli A, Foti S, Passeri F, Ausilio E, Zimmaro P (2018) Local site effects and incremental damage of buildings during the 2016 Central Italy earthquake sequence. *Earthq Spect* 34(4):1639–1669
- Toprak S, Uckan ME, Yilmaz MT et al (2022) Performance of hydraulic structures, lifelines and industrial structures during October 30, 2020 Samos-Aegean sea earthquake. *Bull Earthquake Eng*. <https://doi.org/10.1007/s10518-022-01353-8>
- Triton, Consulting Engineers (2017) Damage repair and reinforcement of the superstructure of the port of Malagari Samos. Final study of port infrastructures, Technical Report, Athens, December 2017

U.S. Geological Survey (2020). Earthquake Hazards Program accessed November 11, 2020, at URL <https://earthquake.usgs.gov/earthquakes/eventpage/us7000c7y0/executive>
 Yakut A, Sucuoğlu H, Binici B, Canbay E, Donmez C, İlki A,... Ay BÖ (2021) Performance of structures in Izmir after the Samos island earthquake. Bull Earthq Eng 1–26

Publisher's Note Springer Nature remains neutral with regard to jurisdictional claims in published maps and institutional affiliations.

Authors and Affiliations

Katerina Ziotopoulou¹ · Kemal Onder Cetin² · Panagiotis Pelekis³ · Selim Altun⁴ · Nikolaos Klimis⁵ · Alper Sezer⁴ · Emmanouil Rovithis⁶ · Mustafa Tolga Yilmaz² · Achilleas G. Papadimitriou⁷ · Zeynep Gulerce² · Gizem Can² · Makbule Ilgac² · Elife Cakır² · Berkan Soylemez² · Ahmed Al-Suhaily² · Alaa Elsaid² · Moutasem Zarzour² · Nurhan Ecemis⁸ · Berna Unutmaz⁹ · Mustafa Kerem Kockar⁹ · Mustafa Akgun¹⁰ · Cem Kincal¹⁰ · Ece Eseller Bayat¹¹ · Pelin Tohumcu Ozener¹² · Jonathan P. Stewart¹³ · George Mylonakis^{14,15} 

✉ George Mylonakis
 g.mylonakis@bristol.ac.uk

¹ University of California Davis, Davis, CA, USA

² Middle East Technical University, Ankara, Turkey

³ University of Patras, Patras, Greece

⁴ Ege University, Bornova, Turkey

⁵ Democritus University of Thrace, Xanthi, Greece

⁶ Institute of Engineering Seismology and Earthquake Engineering, Pilea Chortiatis, Greece

⁷ National Technical University of Athens, Athens, Greece

⁸ Izmir Institute of Technology, Urla, Turkey

⁹ Hacettepe University, Ankara, Turkey

¹⁰ Dokuz Eylul University, Konak, Turkey

¹¹ Istanbul Technical University, Istanbul, Turkey

¹² Yildiz Technical University, Istanbul, Turkey

¹³ University of California Los Angeles, Los Angeles, USA

¹⁴ Khalifa University, Abu Dhabi, United Arab Emirates

¹⁵ University of Bristol, Bristol, UK